Fluid and crystallised intelligence are associated with distinct regionalisation patterns of cortical morphology

C E Palmer[1], W Zhao[2], R Loughnan[2], J Zou[4], C C Fan[1,3], W K Thompson[4], A M Dale[5,6,7] & T L Jernigan[1]

1. Center for Human Development, University of California, San Diego, 9500 Gilman Drive, La Jolla, CA 92161, USA
2. Department of Cognitive Science, University of California, San Diego, 9500 Gilman Drive, La Jolla, CA 92093, USA
3. Center for Multimodal Imaging and Genetics, University of California, San Diego School of Medicine, 9444 Medical Center Dr, La Jolla, CA 92037, USA
4. Division of Biostatistics, Department of Family Medicine and Public Health, University of California, San Diego, La Jolla, CA, USA
5. Department of Radiology, University of California, San Diego School of Medicine, 9500 Gilman Drive, La Jolla, CA 92037, USA
6. Department of Neuroscience, University of California, San Diego School of Medicine, 9500 Gilman Drive, La Jolla, CA 92037, USA
7. Department of Psychiatry, University of California, San Diego School of Medicine, 9500 Gilman Drive, La Jolla, CA 92037, USA

*Corresponding author: Dr. Clare E Palmer (cepalmer@ucsd.edu)

CLASSIFICATION

- MAJOR: Biological sciences
- MINOR: Psychological and cognitive sciences

KEYWORDS: cognition, intelligence, development, adolescence, cortical morphology, regionalisation, neuroimaging

ABSTRACT

Cognitive performance in children is predictive of academic and social outcomes; therefore, understanding neurobiological mechanisms underlying individual differences in cognition during development may be important for improving quality of life. Some theories of intelligence argue that a single latent, psychological construct with a specific neural substrate underlies many cognitive processes. Here we show that a distributed configuration of cortical surface area and apparent thickness, when controlling for global imaging measures, is associated with cognitive performance in a large sample (N=10,145) of nine and ten year old children from the Adolescent Brain and Cognitive Development℠ (ABCD) study. Measures of fluid and crystallised intelligence were associated with strikingly distinct regionalisation patterns of cortical areal expansion and apparent thickness. The minimal overlap in these associations has important implications for competing theories about developing intellectual functions. Importantly, *not* controlling for sociodemographic factors increased the similarity between these regionalisation patterns altering the inferences that would be made. This highlights the importance of understanding the shared variance between sociodemographic factors, cognition and brain structure particularly with a population-based sample such as with ABCD.

SIGNIFICANCE STATEMENT

A lack of statistical power in studies with small sample sizes has hindered research exploring associations between cognitive performance and cortical regionalisation patterns (when controlling for global imaging measures). Using the unprecedented ABCD study® sample, this paper demonstrates that individual variability in the regionalisation of the cortex relates to cognitive function and, importantly, distinct patterns of cortical morphology predict individual differences across different domains of cognitive performance. This heterogeneity highlights that the biology underlying "intelligence" is multifaceted. Moreover, we demonstrate that the sociodemographic diversity within ABCD impacts the association between cortical morphology and cognition similarly across cognitive domains highlighting the importance of understanding how these confounding factors can modify our conclusions regarding the association between brain structure and cognition.

INTRODUCTION

Intelligence is commonly defined using two broad components: fluid and crystallised(1, 2). Fluid intelligence refers to the ability to solve problems, reason, act quickly and adapt to novel situations(1, 3); whereas, crystallised intelligence encompasses task-specific knowledge that accrues throughout the lifespan. Although these factors are seemingly dissociable, they share common variance in hierarchical models of cognition. Indeed, the presence of a positive manifold in correlations of cognitive task performance is one of the most robust findings within psychology: individuals who perform well on a given cognitive task will tend to perform well on many other cognitive tasks(4, 5). The latent factor explaining this shared variance, termed 'g', is predictive of social and academic outcomes(6–8), and is highly heritable(7, 9–11). Previous studies have suggested that 'g' has unique structural and functional neural correlates(12–14); however, these correlates vary greatly across studies, likely due to limited statistical power to identify replicable associations, differences in assessments used to estimate intelligence and differences in neuroimaging processing protocols(15). However, the notion that the shared variance among test scores represents a causal *psychological* construct affecting general intelligence is heavily debated(16, 17). An alternative theory argues that the positive manifold develops through mutually beneficial interactions of independent cognitive processes during development(17, 18). In line with the latter theory, individual differences in cognitive performance would be associated with heterogeneous, distributed neural correlates.

Many studies have measured regional associations between brain structure and cognition; however, these do not always partition out the variance associated with modality-specific global brain measures. Regional differences in cortical morphology relative to total cortical surface area (CSA) or mean cortical thickness (CTH) appear to be important for predicting behaviour (19–23). However, previous studies have been underpowered to detect significant effects of relative cortical configuration across the whole cortex particularly when using univariate statistical methods with stringent control for multiple comparisons (23). Indeed, we know that during embryonic development, regionalisation of areal expansion and apparent cortical thickness occurs via the graded expression of transcription factors across the cortical plate (24, 25). Individual variability in this patterning could therefore result in subtle changes to the whole configuration of the cortex that may impact cognition.

In the current study, we used a multivariate analysis to test the association between the regionalisation of cortical surface area (CSA) and apparent cortical thickness (CTH), relative to global structural measures, in a large sample (n=10,145) of 9 and 10 year old children from the Adolescent Brain and Cognitive Development℠ (ABCD) Study. This large-scale study of 11,880 nine and ten year old children, uses neuroimaging, genetics and a multi-dimensional battery of behavioural assessments to investigate the role of various biological, environmental, and behavioural factors in brain, cognitive, and social/emotional development. Given the biology of cortical development and growing evidence that models encompassing distributed brain-behaviour across the brain better predict behavior (26–28), we used a multivariate approach to assess the significance of the aggregated effect of the brain on behavior across all cortical vertices. We subsequently aimed to examine the degree to which the distributed cortical patterns associating with cognitive performance, namely the fluid and crystallised composite scores from the NIH Toolbox®, exhibited effects of a common underlying architecture or distinct patterns of cortical regionalization.

Importantly, the ABCD Study® sample was recruited to resemble the population of the United States as closely as possible, therefore, the participants are from diverse racial, ethnic and socioeconomic backgrounds. There are large confounding associations between these sociodemographic variables, brain structure and cognitive performance that complicate the interpretation of results. We have therefore performed our analyses with and without controlling for these important sociodemographic variables in order to highlight the implications of this for the interpretation of our findings. This is an important aspect of analysing individual differences in large population-based samples such as the ABCD Study®.

RESULTS

Behavioural data

Figure 1A displays pairwise Pearson correlation coefficients describing the phenotypic relationship between all of the cognitive tasks and the composite scores measured at baseline in the ABCD study. As expected, performance across all tasks was positively correlated. Reading recognition and picture vocabulary performance were most highly correlated with each other (out of the single task measures; r=0.54). These scores were averaged to produce the crystallised composite score, therefore show a high correlation with this measure (r=0.85-0.89). The Toolbox measures used to produce the fluid composite score (flanker, dimensional card sorting, pattern processing speed, picture sequence and list working memory) were less correlated with each other (r=0.19-0.42), therefore showed slightly lower correlations with the fluid composite measure compared to the tasks contributing to the crystallised composite score (r=0.62-0.7). The total composite score (mean of fluid and crystallised) was more highly correlated with the fluid measure (r=0.91) compared to the crystallised measure (r=0.79).

Figure 1B shows the same correlation matrix after pre-residualising all of the cognitive measures for the covariates of no interest (age, sex, race/ethnicity, household income and parental education) in order to show the phenotypic correlations after controlling for these confounding factors. Most of the correlation coefficients decreased in this analysis; however, the overall pattern of these relationships remained consistent.

Determining the association between the regionalisation of cortical morphology and cognition

We used a multivariate statistical omnibus test (MOSTest)(28) to measure the association between the regionalisation of CSA and CTH and individual differences in cognitive performance on the fluid and crystallised composite scores from the NIH Toolbox. This multivariate approach aggregates effects across the entire cortex and therefore is better able to detect associations that are distributed compared to a standard univariate neuroimaging omnibus test that assumes effects are sparse and localised. The MOSTest also takes into account the covariance across the brain. This statistical procedure implements a permutation test with 10,000 permutations to determine statistical significance. For all associations the observed multivariate statistic fell beyond the null distribution of permuted statistics ($p<0.0001$; Table 1). To calculate a more precise p-value for the associations we extrapolated beyond the null distribution (see Supplementary Methods). All associations were also significant when using more widely used univariate omnibus statistic (Min-

P; p<0.0005), but were smaller in magnitude than when using the MOSTest. This suggests that the distributed signal across the cortex may be important for predicting cognitive performance. The regionalisation of CTH showed greater associations with cognitive performance than CSA. All of these analyses controlled for all sociodemographic factors (race/ethnicity, household income and parental education) as well as age, sex and scanner ID. In addition, we measured all associations using two alternative multivariate statistics, Stouffer and Fisher, to determine method invariance of these brain-behavior associations. All of these methods converged (supplementary figure 1).

	Permuted P-values		***Extrapolated P-values***	
	Min-P	**MOST**	**Min-P**	**MOST**
CSA ~ fluid score + covariates	5.00E-04	1.00E-04	1.29E-04	2.93E-10
CSA ~ crystallised score + covariates	1.00E-04	1.00E-04	9.34E-06	1.53E-07
CTH ~ fluid composite score + covariates	1.00E-04	1.00E-04	3.96E-05	5.59E-19
CTH ~ crystallised score + covariates	2.00E-04	1.00E-04	4.13E-08	8.71E-18

Table 1. Cortical morphology was significantly associated with both fluid and crystallised composite scores. Permuted p-values demonstrate statistical significance based on the rank of the observed statistic in the distribution of permuted statistics. For all associations both the observed univariate (min-P) and multivariate (MOST) test statistics were in the extreme of the respective null distributions, therefore we rejected the null hypothesis that the observed statistics came from the empirical null distribution. Extrapolated p-values provide an estimate of the likelihood of the observed statistics beyond the range that can be directly estimated from the permutations. The magnitude of effects were larger using the multivariate test statistic and for associations between cognitive performance and CTH (controlling for mean CTH).

Distinct patterns of association between the regionalisation of CSA and the fluid and crystallised composite scores

After establishing significant associations between cortical morphology and cognitive performance, we aimed to measure the similarity across the estimated effect size maps for these associations. Interestingly, on visualising the estimated effect size maps of the associations between the regionalisation of CSA (controlling for total CSA) and the fluid and crystallised composite scores, we saw a unique structural pattern of association for each composite score (Fig 2A&B). Figure 2C shows the difference between the beta coefficients for the fluid (F) and crystallised (C) surface maps. To quantify the magnitude of these vertex-wise differences relative to the original associations, we calculated a ratio of the variance (root mean squared) of the beta coefficient differences divided by the variance (root mean squared) of the average beta coefficients across the F and C estimated effect size maps (RMS ratio for F − C = 1.21).

In order to determine the unique pattern of association between the relative configuration of CSA and the fluid and crystallised composite scores, we generated a vertex-wise association map between the regionalisation of CSA and the fluid composite score controlling for the crystallised composite score (F_C; figure 2E), and the crystallised composite score controlling for the fluid composite score (C_F; figure 2H). The pattern of associations was almost identical to that obtained when the respective composite score was not included as a covariate in the model. Indeed, the surface map of the vertex-wise differences between the associations for each composite score and

that composite score controlling for the other were very small in magnitude compared to the original F - C effect size maps (figure 2F,I; RMS ratio for $C - C_F = 0.27$; RMS ratio for $F - F_C = 0.38$).

Moreover, the vertex-wise correlation between the estimated beta coefficients for F vs F_C was high (r=0.92) as was the correlation between the beta coefficients for C vs C_F (r=0.95). In contrast, the vertex-wise correlation between the beta coefficients for F vs C was much lower (r=0.30). This further implies that there was minimal shared variance between the associations for the fluid and crystallised scores and the regionalisation of CSA. The minimal overlap in the cortical configuration associated with these measures supports that the configurations of relative CSA associated with these measures were relatively distinct.

Distinct patterns of association between the regionalisation of CTH and the fluid and crystallised composite scores

Estimated effect size maps showing the vertex-wise associations between the relative configuration of CTH and the fluid and crystallised composite scores are shown in figure 3A&B. The structural pattern of association between these composite scores and CTH were more similar than with CSA. However, there were still key regions with distinct differences in relative CTH associations between the fluid and crystallised composite scores. Figure 3C shows the difference between the beta coefficients for the F and C surface maps, which were relatively large compared to the original estimated effect sizes (RMS ratio for $F - C = 0.92$). In order to determine the unique pattern of association between the regionalisation of CTH and F and C, we generated a vertex-wise map of the association between the regionalisation of CTH and F_C (figure 3E) and CTH and C_F (figure 3H). As with CSA, the pattern of associations was almost identical to when the respective intelligence measure was not included in the model. Indeed, the estimated effect size map of the vertex-wise differences between the associations for each composite score and each composite score controlling for the other were very small in magnitude (figure 3F,I; RMS ratio for $C - C_F = 0.31$; RMS ratio for $F - F_C = 0.30$). The vertex-wise correlations between the map of associations for each composite score and that composite score controlling for the other were high (F vs F_C: r=0.94; C vs C_F: r=0.95); whereas the vertex-wise correlation between the maps of association for the fluid and crystallised composite scores was much lower (F vs C: r=0.40). As with CSA, the minimal overlap in the cortical configurations associated with these measures supports that the configurations of CTH associated with these measures were relatively distinct.

Distinct patterns of association for the regionalisation of CTH and CSA across cognitive tasks

Visualising the effect size maps between each cortical measure and each cognitive task revealed relatively distinct patterns of association across the cognitive tasks (figure 4). This was further supported by the low vertex-wise correlations across these associations (figure 5). The estimated beta coefficients for the regionalisation of CTH and cognition were more correlated across tasks than for the regionalisation of CSA and cognition. Effect size maps were more similar for tasks using similar underlying cognitive processes and the composite measures appeared to reflect mixtures of the patterns of association for each of the tasks that were averaged to produce the composite scores. Estimated effect size maps for each cortical measure and each cognitive task and composite score without controlling for the sociodemographic variables of race/ethnicity,

household income and parental education were more highly correlated (figure 5C&D). This shows that variance in the sociodemographic factors is shared with the cognitive and structural measures.

Association maps when not controlling for sociodemographic variables

We computed the estimated effect size maps for the F and C composites scores associated with the regionalisation of CSA (figure 6A&B) and CTH (figure 6D&E) without controlling for the sociodemographic variables. For both morphology measures, the vertex-wise correlation between the F and C maps increased (CSA: r=0.69; CTH: r=0.89). However, the F-C difference maps were remarkably similar to when the sociodemographic variables were controlled for as shown by a vertex-wise correlation between the F-C difference maps with and without controlling for sociodemographic factors (CSA: r=0.96; CTH: r=0.94). This strongly suggests that these confounding variables in aggregate index common shared variance between cortical morphology and cognition across domains that is not specific to a particular task performance. Estimated effect size maps for the association between the regionalisation of CSA and CTH and cognitive performance across tasks without controlling for sociodemographic factors can be found in supplementary figure 3.

Partitioning the variance between brain structure and cognition

In order to quantify the variance in each cognitive phenotype predicted by the vertex-wise imaging data for the regionalisation of CSA and CTH, we calculated a polyvertex score (PVS). Much like a polygenic risk score, the PVS represents a linear weighted sum of the vertex-wise associations, which are projected from a training set to an independent hold-out set within a cross validation framework. A comparison of the subject-wise PVS with cognitive performance, therefore provides a conservative, lower-bound estimate of the unique variance in behavior predicted by the regionalisation of cortical morphology independent of the global brain measures. The regionalisation of CSA explained a similar proportion of the total variability in cognition compared to the regionalisation of CTH (for fluid scores: total CSA = ~2.59%R^2; CSA PVS = ~1.27%R^2; CTH PVS =~1.88%R^2; for crystallised scores: total CSA predicted ~7.15%R^2; CSA PVS predicted ~2.39%R^2; CTH PVS = ~3.85%R^2; figure 7). Mean CTH was not predictive of cognitive performance. Total CSA predicted more variance in crystallised scores than fluid scores. Across imaging measures the sociodemographic variables accounted for ~70-90% of the variation in fluid and crystallised scores predicted by brain structure. Without controlling for brain structure, the sociodemographic factors collectively predicted more variance in crystallised (~23%R^2) compared to fluid scores (~10%R^2). CTH measures (mean CTH and CTH PVS) explained ~22% of the association between the sociodemographic variables and the crystallised score and ~27% for the fluid score, whilst CSA (total CSA and CSA PVS) explained ~37% of the association between the sociodemographic variables and the crystallised score and ~44% for the fluid score. This shows that the relationship between brain structure and cognition was strongly related to the sociodemographic factors.

DISCUSSION

In this study, we have shown that the regionalisation of cortical morphology, independent of global brain measures, was significantly associated with individual differences in cognitive performance in

a large sample of 9 and 10 year old children (N=10,145). Moreover, we showed that individual differences in estimates of fluid and crystallised intelligence were associated with distinct maps of relative cortical areal expansion and apparent thickness. This suggests that regional cortical architecture is related differently to these two types of cognitive function. The relatively distinct association maps for the single tasks used to generate these composite measures provides evidence in support of mutualism or sampling models of intelligence, which argue that no single, latent neural construct is required to account for the strong positive manifold underlying "g". Furthermore, we have shown that the sociodemographic diversity within ABCD impacts the association between cortical morphology and cognition similarly across cognitive domains. Since the treatment of sociodemographic variables in these models led to substantial differences in the magnitude of effects of interest, users of ABCD data should select covariates carefully and discuss any sociodemographic factors potentially related to both explanatory variables and outcomes.

Relative cortical configuration is important for cognition

Global brain measures have been previously associated with cognition; however, there are many examples where there are differences in global brain measures, such as brain size between men and women, which do not correspond with differences in cognition. When measuring regional associations with behaviour it is therefore essential to control for these global measures in order to uncover specific relationships between regionalisation and behaviour. Indeed, a number of studies have highlighted associations between regional differences in cortical morphology and cognition; however, they have lacked the power to measure associations based on the entire configuration of cortical morphology. Importantly, the regionalisation of CSA and CTH has been associated with distinct, continuous gradients of genetic influences across the cortex (29–31) that coincide with the gene expression patterns that dictate specialisation of the neocortex during embryonic development (24, 25). Individual differences in this molecular signalling could therefore lead to subtle alterations in this cortical configuration, which could lead to variability in behaviour. Here we have used a multivariate statistical approach to measure the significance of distributed effects, which reflect the graded and distributed nature of the biology of regionalisation.

We have shown that performance across multiple cognitive tasks was associated with the regionalisation of cortical morphology across the whole cortex. For both morphology measures, there was a clear pattern of positive and negative associations with cognitive performance, which suggests that, at this developmental stage, *relative* differences in the size and thickness of cortical regions mirror individual difference variability in cognition. Indeed, the regionalisation of CSA predicted additional unique variance in cognition not explained by total CSA. By partitioning the variance in this way, we can determine the relative importance of these components of CSA for cognition. This appeared to differ depending on the cognitive task, with more crystallised measures having a greater association with total CSA compared to the regionalisation of CSA. Comparatively the proportion of variance in behaviour explained by regional CTH was relatively similar for fluid and crystallised measures. Mean CTH did not predict cognitive performance across any measures; however this may be due to the developmental stage of this sample.

Distinct associations between cortical morphology and different cognitive modalities

The estimated effect size maps between the regionalisation of CSA and the crystallised composite score (comprised of reading and vocabulary measures) showed that greater areal expansion in

regions previously associated with language functions, such as the left temporal and middle frontal regions(32–34), was associated with higher crystallised scores; whereas, greater areal expansion in a different set of regions, previously implicated in cognitive control mechanisms required for the fluid tasks, such as the anterior cingulate and insula cortices(19, 20, 35–37), was associated with higher fluid scores. The patterns of apparent CTH associated with these measures were slightly less distinct, however to some degree appeared to mirror these associations with areal expansion.

Interestingly, the areas most strongly associated with the total composite score were a combination of those most strongly associated with either fluid or crystallised intelligence. The maps of association between both the regionalisation of CSA and CTH and the total composite score represent a mixture of the fluid and crystallised associations. Indeed, the same can be seen for the fluid and crystallised composite score maps, which appear to represent a mixture of the association maps for each of the individual tasks that contributed to those scores. This is reflected within the correlation matrix of the vertex-wise associations (figure 5A&B). This observation has important implications for theories of intelligence.

Theories of intelligence: sampling, mutualism or 'g'?

Factor analyses of cognitive measures frequently reveal a higher order general latent factor 'g' that can explain (statistically) individual differences in cognitive performance. However, this observation alone does not necessarily reveal anything about the origins or development of 'g'. Here we clearly do not observe a single, causal neuroanatomical substrate that may represent 'g' (i.e., influence performance on all cognitive tasks). Brain size is frequently associated with "general cognitive ability" and thought to represent 'g'. Indeed total CSA was modestly associated with cognitive performance in the current study; however, before controlling for demographic factors, total CSA only predicted ~7% of the variability in crystallised scores and ~2% in fluid scores. Due to the unprecendented statistical power in this study, we can infer that total CSA is unlikely, across other studies, to account for any more individual variability in cognitive scores in children of this age. Indeed, this effect is much smaller than the shared variance across cognitive measures that has been attributed to 'g' (~21%) in a similar sample from the ABCD study(38). Moreover, the relative importance of this measure for predicting individual variability in cognition differed as a function of the type of intelligence measured, which is inconsistent with this being a global effect. These results do not rule out that a single or global neural phenotype underlying intelligence could be represented within a different neural modality, such as functional connectivity or latency of neuronal signalling; however, there is a lack of supporting evidence for a dominant neural 'g' phenotype in the current study. There are alternative models of intelligence that attempt to explain how the positive manifold (the positive correlation across cognitive tasks) can be generated from multiple, independent psychological constructs, which fit more in line with the results shown here.

The sampling model posits that because cognitive tasks do not measure a single cognitive process, but instead require multiple processes, the overlap in the processes required across similar tasks produces a positive correlation between them(39, 40). An alternative mutualism model simulates the positive manifold via mutually beneficial interactions between initially uncorrelated systems that support cognitive behaviours(17, 18). For example, having good short-term memory may aid the development of cognitive strategies, which can in turn lead to better short-term memory(41). In this model, each initially independent system has a biological constraint, or resource, which limits the potential growth of that system. These resources may be determined by either genetics or the

environment, or both, and confer individual differences in how these systems develop and interact over time. The weighted sum of these resources, in simulations using the mutualism model, is a good predictor of cognitive performance and correlates highly with the 'g' that emerges from mutualism. This is an important distinction from the more conventional 'g' model as here individual differences in mature cognitive performance emerge from different combinations of these resources. For example, the same IQ score could arise from high memory resources in one individual, but high processing speed in another individual.

In the current study, the configuration of cortical morphology associated with the total composite score (our proxy for 'g') appeared to be a mixture (weighted sum) of structural associations with the other cognitive tasks. In turn, each of these tasks clearly does not represent a single cognitive process, but requires a different combination of many cognitive processes. Here we suggest that relative differences in cortical morphology may reflect to some degree the scaffolding, or resources, contributing to the performance of these processing systems, and different mixtures of these configurations may map to different levels of performance on each cognitive task.

Understanding individual variability in cognition related to both brain structure and sociodemographic factors

Before controlling for sociodemographic variables, the proportion of variance in the composite measures of cognitive performance shared with the brain phenotypes was ~9% for the crystallised scores and ~4% for the fluid scores. Overall, these phenotypes and the partially confounded sociodemographic variables together accounted statistically for ~32% of the variance in crystallised scores and ~20% of the variance in fluid scores. These results suggest that many factors that relate to individual differences in cognitive test scores remain unaccounted for in these statistical models. However, the results are sufficiently powerful to constrain future hypotheses by restricting the range of plausible causal effects of well-measured variables, such as total CSA.

The cortical arealisation phenotype and regionalisation of apparent CTH both accounted for additional unique variance in cognition independent of global measures. Even after pre-residualising for sociodemographic factors that could index cultural, environmental and other experiential effects on cognitive test scores, as well as global brain measures, the associations between the cortical regionalisation phenotypes and cognitive test scores were statistically robust; but only explained ~0.1% of the residual variation. Here we have used a very conservative, out-of-sample effect size; we are therefore providing the lower bound for the estimated effect size between regionalisation and cognition, which is not influenced by any confounding measures. These effects may be very small, but that is perhaps not surprising given the number of factors that can influence cognition and is common-place among samples of this size where effect sizes are not inflated by sampling variability or publication bias. Our results show that the sociodemographic variables accounted for a substantial proportion of the shared variance between the brain phenotypes and composite measures of cognitive function. This may result from many small effects of factors indexed by these variables, such as nutrition, limited access to healthcare and education, untreated prenatal complications, high levels of stress or exposure to environmental toxins.

It is possible that the dissociable, specific variance across cognitive domains associated with cortical regionalisation, after controlling for sociodemographic factors, is mediated by genetic variability in cortical arealisation. Indeed, the regionalisation of the cortex is moderately

heritable(42–44) and during early embryonic development, gradients of morphogens dictate the expression of transcription factors across the dorsal proliferative zone, which determines the eventual spatial location and functional specialisation of cortical projection neurons(24, 25). Such biases in arealisation may influence developing cognitive functions in an individual in ways that advantage some functional domains relative to others, which creates important diversity within our population. The brain-behaviour associations in the current study most likely reflect both genetically mediated differences in cortical architecture and both independent and correlated interactions with the environment and other developing brain systems. Indeed, within our education system, particular individuals may be selectively advantaged and thus may be disproportionately exposed to environments that can enhance the positive interactions between developing systems, multiplying a specific genetic effect. This gene-environment correlation can inflate heritability estimates and increase individual variability in estimates of general intelligence(45–48).

Given our current findings, we hypothesise that it is unlikely that there is a single cortical configuration underlying general intelligence; however, there may be a dominant phenotype, or configuration of resources (shown here as the mean association pattern), that may offer an advantage in our society and be selected for by our education system. Subsequent analyses are required to directly test this hypothesis by quantifying the heterogeneity in cortical architecture across this sample and determining if there are different clusters of individuals within the sample with different cortical configurations that are associated with the same cognitive performance. This will provide increased support for mutualism models of intelligence in which variability in the configuration (weighting) of resources across individuals can result in similar levels of general intelligence. This may also explain why the mean association maps explain a very small proportion of variability in behaviour.

Conclusions

The graded and distributed nature of the neurobiology underlying the regionalisation of the cortex supports the importance of studying the whole configuration of cortical morphology associated with behaviour using multivariate statistics and continuous pattern comparison methods. Using the unprecedented ABCD dataset, we now have the power to discover novel brain-behaviour associations and understand individual variability in behaviour among a diverse sample of participants. With future releases of the ABCD data we will track how the regionalisation of CSA and CTH and cognitive performance change over time within an individual to further understand these relationships.

Materials & Methods

Sample

The ABCD study is a longitudinal study across 21 data acquisition sites enrolling 11,880 children starting at 9 and 10 years old. This paper analysed the baseline sample from release 2.0.1 (NDAR DOI: 10.15154/1504041). The ABCD Study used school-based recruitment strategies to create a population-based, demographically diverse sample, however it is not necessarily representative of the U.S. national population (49, 50). Due to the inclusion of a wide range of individuals across different races, ethnicities and socioeconomic backgrounds, it is important to carefully consider how to control for these potentially confounding factors and the implications of this on our effects of interest. Sex and age were used as covariates in all analyses. Only subjects who had complete data across all of the measures analysed were included in the neuroimaging analyses creating a final sample of 10,145 subjects. Full sample details can be found in the Supplementary Material. Supplementary Table 1 displays the names of each variable used in these analyses from data release 2.0.1. Supplementary Table 2 shows the demographic characteristics of the sample as a function of cognitive performance.

Neurocognitive assessment

The ABCD Study neurocognitive assessment at baseline consisted of the NIH Toolbox Cognition Battery® (NIHTBX), the WISC-V matrix reasoning task, the Little Man Task (LMT) and the Rey Auditory Verbal Learning task (RAVLT). All of the tasks were administered using an iPad with support or scoring from a research assistant where needed. The NIHTBX is a widely used battery of cognitive tests that measures a range of different cognitive domain. It includes an the Toolbox Oral Reading RecognitionTask® (TORRT), Toolbox Picture Vocabulary Task® (TPVT), the Toolbox Pattern Comparison Processing Speed Test® (TPCPST), Toolbox List Sorting Working Memory Test® (TLSWMT), Toolbox Picture Sequence Memory Test® (TPSMT), Toolbox Flanker Task® (TFT) and Toolbox Dimensional Change Card Sort Task® (TDCCS). Details of each task can be found in the supplementary materials. In the current study, the uncorrected scores for each task were used for statistical analyses. Composite scores of crystallised intelligence (mean of TPVT and TORRT), fluid intelligence (mean of TPCPST, TLSWMT, TPSMT, TFT and TDCCS) and total score (mean of all tasks) were also analysed. These measures are highly correlated with 'gold standard' measures of intelligence in adults(52) and children(53).

MRI acquisition & Image pre-processing

The ABCD MRI data were collected across 21 research sites using Siemens Prisma, GE 750 and Philips 3T scanners. Scanning protocols were harmonised across sites. Scanner ID was included in all analyses to control for any differences in image acquisition across sites and scanners. Full details of all the imaging acquisition protocols used in ABCD are outlined by Casey et al (59). Pre-processing of all MRI data for ABCD was conducted using in-house software at the Center for Multimodal Imaging and Genetics (CMIG) at University of California San Diego (UCSD) as outlined in Hagler et al (60). Cortical surfaces were constructed from T1-weighted structural images for each subject and segmented to calculate measures of apparent cortical thickness and surface area using FreeSurfer v5.3.0(61–65). Cortical maps were smoothed using a Gaussian kernel of 20 mm full-

width half maximum (FWHM) and mapped into standardised spherical atlas space. Vertex-wise data for all subjects for each morphometric measurement were concatenated into matrices in MATLAB R2017a and entered into general linear models for statistical analysis using custom written code. More details can be found in the Supplementary Materials.

Statistical Analysis

Vertex-wise effect size maps

All behavioural variables were standardised (z-scored) prior to analysis as was the vertex-wise brain data. We applied a general linear model (GLM) univariately at each vertex (n=1284) associating a given behaviour from a set of covariates (age, sex, scanner ID, race/ethnicity, household income and parental education) and the vertex-wise morphology data. Mass univariate standardised beta surface maps were created showing the vertex-wise associations for each analysis. Vertexwise effect size maps were calculated for all of the thirteen cognitive measures predicted by relative CSA (controlling for total CSA) and relative CTH (controlling for mean CTH) separately resulting in N=26 independent vertex-wise analyses. Models determining the association between CSA and behaviour included total CSA (sum of CSA across vertices) as an additional predictor and models analysing CTH included the mean CTH across vertices. These analyses were repeated with and without including race/ethnicity, income and parental education covariates.

Determining the significance of the effect size maps using an omnibus test

In order to determine whether there was a significant association between vertex-wise cortical morphology (controlling for global measures) and cognitive task performance, we employed a permutation test using a univariate statistic (min-p) and three multivariate statistics (MOSTest, Stouffer and Fisher). Using the least-squares estimates β_v from each GLM at each vertex, we computed the $V \; x \; 1$ vector of Wald statistics $\boldsymbol{z} = (z, \ldots, z_V)'$ across the whole cortex and accompanying p-values: $p = \; 2normcdf(-|z|)$. Using these values we calculated 4 different test statistics for the permutation test outlined in Table 2.

Univariate	Tippett (Min-P)	min (p)
Multivariate	MOSTest	$z'\widehat{\boldsymbol{R}}^{-1}z$
Multivariate	Fisher	$-2\sum \ln(p)$
Multivariate	Stouffer	$\sum \lvert z \rvert / \sqrt{V}$

Table 2. Univariate and multivariate test statistics measured.

The univariate statistic, min-P was defined as the most significant (smallest) p-value across the cortex. This is commonly used neuroimaging omnibus test, but does not take into account the distributed nature of many brain-behavior associations. The multivariate omnibus test (MOSTest)(28) is a more pertinent omnibus test as it determines the significance of the whole pattern of effects across the cortex taking into account the covariance structure across vertices. χ^2_{MOST} was calculated as the estimated squared Mahalanobis norm of $\boldsymbol{z}$. The Fisher and Stouffer

methods are additional alternative multivariate methods for aggregating effects across the cortex, but do not take into account the covariance across vertices. These are likely less optimal statistics, but do not rely on the regularisation of a high dimensional matrix, therefore were included to show convergence of results across multiple methods.

To correctly estimate the null distribution from permutations, subject labels were shuffled according to exchangeability blocks (EBs) defined based on the family structure within ABCD (66). This permutation procedure was used to determine the distribution of each test statistic under the global null hypothesis H_0. We rejected H_0 if the observed test statistic was greater than the value of the permuted test statistic at the critical threshold corresponding to an alpha level of 0.0038 (0.05 corrected for the 13 cognitive tests analysed).

Comparison across associations maps

To determine the shared variance between the effect size maps for the fluid (F) and crystallised (C) composite scores for each imaging phenotype, additional maps were created controlling for the other composite measure by including that measure as an additional covariate within the design matrix. This produced a vertexwise standardised beta effect size surface map for F independent of the association between cortical morphology and C (F_C) and C independent of F (C_F). Surface maps of the difference between the vertexwise beta coefficients as well as vertexwise Pearson correlation coefficients were calculated for the following contrasts: $F - C$, $F - F_C$ and $C - C_F$. The magnitude of effects across the cortex for each map was calculated using the following formula: $= \sqrt{\overline{\beta^2}}$. In order to determine the relative size of the effects across the difference maps compared to the individual maps we calculated an RMS ratio using the following formula: $RMS_{DIFF}/(\frac{RMS_1+RMS_2}{2})$, with RMS_{DIFF} representing the RMS of the difference map and RMS1 and RMS2 as the RMS for each individual map used to produce the difference.

Quantifying the magnitude of the association between brain structure and cognition using a polyvertex score (PVS)

The PVS was calculated for the fluid and crystallised composite scores to quantify the behavioural variance explained by the vertex-wise cortical morphology. All behavioural and imaging data were pre-residualised using the covariates of no interest prior to calculation of the PVS. We completed this step multiple times including different covariates in order to determine the change in R^2 when particular demographic variables were and were not controlled for.

For the imaging data, we included the global CSA and CTH measures specific to each modality in the pre-residualisation as covariates. This allowed us to determine the unique association between relative cortical morphology and cognition and compare this to the predictive power of brain structure without controlling for global measures. The method used here is the univariate PVS method outlined in detail by Zhao and colleagues(26). The association between the imaging phenotype and behaviour across the whole sample was calculated as the squared correlation (R^2) between the observed behaviour and the predicted behaviour (the PVS). In order to explore the proportion of shared variability in cognitive performance explained by brain structure and the demographic variables, we generated several linear models with differing predictors. These models were generated separately for each imaging modality (when these were included) and with

either the fluid or crystallised scores as the dependent variable. Each model was trained on 90% of the sample and tested in a 10% hold out set within a 10-fold cross validation framework to produce a robust, out-of-sample R^2. The models are outlined in figure 7.

Acknowledgements

The authors wish to thank the youth and families participating in the Adolescent Brain Cognitive Development (ABCD) Study and all ABCD staff. Data used in the preparation of this article were obtained from the Adolescent Brain Cognitive Development (ABCD) Study (https://abcdstudy.org), held in the NIMH Data Archive (NDA). This is a multisite, longitudinal study designed to recruit more than 10,000 children age 9-10 and follow them over 10 years into early adulthood. The ABCD Study is supported by the National Institutes of Health and additional federal partners under award numbers U01DA041022, U01DA041028, U01DA041048, U01DA041089, U01DA041106, U01DA041117, U01DA041120, U01DA041134, U01DA041148, U01DA041156, U01DA041174, U24DA041123, U24DA041147, U01DA041093, and U01DA041025. A full list of supporters is available at https://abcdstudy.org/federal-partners.html. A listing of participating sites and a complete listing of the study investigators can be found at https://abcdstudy.org/Consortium_Members.pdf. ABCD consortium investigators designed and implemented the study and/or provided data but did not all necessarily participate in analysis or writing of this report. This manuscript reflects the views of the authors and may not reflect the opinions or views of the NIH or ABCD consortium investigators. The ABCD data repository grows and changes over time. The data was downloaded from the NIMH Data Archive ABCD Collection Release 2.0.1 (DOI: 10.15154/1504041).

REFERENCES

1. J. L. Horn, R. B. Cattell, Refinement and test of the theory of fluid and crystallized general intelligences. *J. Educ. Psychol.* **57**, 253–270 (1966).
2. I. J. Deary, Intelligence. *Annu. Rev. Psychol.* **63**, 453–482 (2012).
3. T. A. Salthouse, When does age-related cognitive decline begin? *Neurobiol. Aging* **30**, 507–514 (2009).
4. C. Spearman, "General Intelligence," Objectively Determined and Measured. *Am. J. Psychol.* **15**, 201 (1904).
5. D. Wechsler, *The measurement of adult intelligence (3rd ed.).* (Williams & Wilkins Co, 1946) https:/doi.org/10.1037/11329-000.
6. D. M. Cutler, A. Lleras-Muney, D. Cutler, A. Lleras-Muney, Education and Health: Insights from International Comparisons (2012) (August 26, 2019).
7. L. S. Gottfredson, I. J. Deary, "Intelligence Predicts Health and Longevity, but Why?" (2004).
8. Arendt, J. Nielsen, Does education cause better health? A panel data analysis using school reforms for identification. *Econ. Educ. Rev.* **24**, 149–160 (2005).
9. M. S. Panizzon, *et al.*, Genetic and Environmental Influences of General Cognitive Ability: Is g a valid latent construct? *Intelligence* **43**, 65 (2014).
10. T. Bouchard, M. McGue, Familial studies of intelligence: a review. *Science (80-.).* **212**, 1055–1059 (1981).
11. R. Plomin, F. M. Spinath, Intelligence: Genetics, Genes, and Genomics. *J. Pers. Soc. Psychol.* **86**, 112–129 (2004).
12. R. Colom, *et al.*, Neuroanatomic overlap between intelligence and cognitive factors: Morphometry methods provide support for the key role of the frontal lobes. *Neuroimage* **72**, 143–152 (2013).
13. R. Colom, *et al.*, Gray matter correlates of fluid, crystallized, and spatial intelligence: Testing the P-FIT model. *Intelligence* **37**, 124–135 (2009).
14. M. Burgaleta, W. Johnson, D. P. Waber, R. Colom, S. Karama, Cognitive ability changes and dynamics of cortical thickness development in healthy children and adolescents. *Neuroimage* **84**, 810–819 (2014).
15. K. Martínez, *et al.*, Reproducibility of brain-cognition relationships using three cortical surface-based protocols: An exhaustive analysis based on cortical thickness. *Hum. Brain Mapp.* **36**, 3227–3245 (2015).
16. R. Sternberg, E. Grigorenko, *The general factor of intelligence* (Mahwah, NJ, US: Lawrence Erlbaum Associates Publishers, 2002).
17. H. L. J. Van Der Maas, *et al.*, A Dynamical Model of General Intelligence: The Positive Manifold of Intelligence by Mutualism (2006) https:/doi.org/10.1037/0033-295X.113.4.842.
18. H. Van Der Maas, K.-J. Kan, M. Marsman, C. E. Stevenson, Network Models for Cognitive Development and Intelligence. *J. Intell.* **5**, 16 (2017).

19. A. M. Fjell, *et al.*, Multimodal imaging of the self-regulating developing brain. *Proc. Natl. Acad. Sci. U. S. A.* **109**, 19620–19625 (2012).

20. L. B. Curley, *et al.*, Cortical morphology of the pars opercularis and its relationship to motor-inhibitory performance in a longitudinal, developing cohort. *Brain Struct. Funct.* **223**, 211–220 (2018).

21. E. Newman, *et al.*, Anxiety is related to indices of cortical maturation in typically developing children and adolescents. *Brain Struct. Funct.* **221**, 3013–3025 (2016).

22. E. Newman, *et al.*, Go/No Go task performance predicts cortical thickness in the caudal inferior frontal gyrus in young adults with and without ADHD. *Brain Imaging Behav.* **10**, 880–892 (2016).

23. E. Vuoksimaa, *et al.*, Is bigger always better? The importance of cortical configuration with respect to cognitive ability. *Neuroimage* **129**, 356–366 (2016).

24. D. D. M. O'Leary, S. J. Chou, S. Sahara, Area patterning of the mammalian cortex. *Neuron* **56**, 252–269 (2007).

25. P. Rakic, A. E. Ayoub, J. J. Breunig, M. H. Dominguez, Decision by division: making cortical maps. *Trends Neurosci.* **32**, 291–301 (2009).

26. W. Zhao, *et al.*, The Bayesian polyvertex score (PVS-B): a whole-brain phenotypic prediction framework for neuroimaging studies. *bioRxiv*, 813915 (2019).

27. M. C. Reddan, M. A. Lindquist, T. D. Wager, Effect size estimation in neuroimaging. *JAMA Psychiatry* **74**, 207–208 (2017).

28. D. van der Meer, *et al.*, Understanding the genetic determinants of the brain with MOSTest. *Nat. Commun.* **11**, 1–9 (2020).

29. C.-H. Chen, *et al.*, Genetic Influences on Cortical Regionalization in the Human Brain. *Neuron* **72**, 537–544 (2011).

30. C.-H. Chen, *et al.*, Genetic topography of brain morphology. *Proc. Natl. Acad. Sci.* **110**, 17089–17094 (2013).

31. C. Chen, *et al.*, Hierarchical Genetic Organisation of Human Cortical Surface Area. **335**, 1634–1636 (2013).

32. G. Hickok, D. Poeppel, The cortical organization of speech processing. *Nat. Rev. Neurosci.* **8**, 393–402 (2007).

33. A. Martin, M. Schurz, M. Kronbichler, F. Richlan, Reading in the brain of children and adults: a meta-analysis of 40 functional magnetic resonance imaging studies. *Hum. Brain Mapp.* **36**, 1963–1981 (2015).

34. W. E. Brown, *et al.*, Preliminary evidence of widespread morphological variations of the brain in dyslexia. *Neurology* **56**, 781–3 (2001).

35. M. M. Botvinick, J. D. Cohen, C. S. Carter, Conflict monitoring and anterior cingulate cortex: an update. *Trends Cogn. Sci.* **8**, 539–546 (2004).

36. V. Menon, L. Q. Uddin, Saliency, switching, attention and control: a network model of insula function. *Brain Struct. Funct.* **214**, 655–667 (2010).

37. K. S. Taylor, D. A. Seminowicz, K. D. Davis, Two systems of resting state connectivity between the insula and cingulate cortex. *Hum. Brain Mapp.* **30**, 2731–2745 (2009).

38. W. K. Thompson, *et al.*, The structure of cognition in 9 and 10 year-old children and associations with problem behaviors: Findings from the ABCD study's baseline neurocognitive battery. *Dev. Cogn. Neurosci.* **36** (2019).

39. D. J. Bartholomew, I. J. Deary, M. Lawn, A new lease of life for Thomson's bonds model of intelligence. *Psychol. Rev.* **116**, 567–79 (2009).

40. K. Kovacs, A. R. A. Conway, Process Overlap Theory: A Unified Account of the General Factor of Intelligence. *Psychol. Inq.* **27**, 151–177 (2016).

41. R. Siegler, E. A. Jenkins, E. A. Jenkins, *How Children Discover New Strategies* (Routledge, 1989) https:/doi.org/10.4324/9781315807744 (August 22, 2019).

42. L. T. Eyler, *et al.*, Genetic and environmental contributions to regional cortical surface area in humans: A magnetic resonance imaging twin study. *Cereb. Cortex* **21**, 2313–2321 (2011).

43. L. T. Eyler, *et al.*, A comparison of heritability maps of cortical surface area and thickness and the influence of adjustment for whole brain measures: A magnetic resonance imaging twin study. *Twin Res. Hum. Genet.* **15**, 304–314 (2012).

44. A. M. Winkler, *et al.*, Cortical thickness or grey matter volume? The importance of selecting the phenotype for imaging genetics studies. *Neuroimage* **53**, 1135–1146 (2010).

45. W. T. Dickens, J. R. Flynn, Heritability estimates versus large environmental effects: the IQ paradox resolved. *Psychol. Rev.* **108**, 346–69 (2001).

46. K.-J. Kan, J. M. Wicherts, C. V. Dolan, H. L. J. van der Maas, On the Nature and Nurture of Intelligence and Specific Cognitive Abilities. *Psychol. Sci.* **24**, 2420–2428 (2013).

47. R. J. Loughnan, *et al.*, Polygenic Score of Intelligence is More Predictive of Crystallized than Fluid Performance Among Children. *bioRxiv*, 637512 (2019).

48. K. P. Harden, E. Turkheimer, J. C. Loehlin, Genotype by environment interaction in adolescents' cognitive aptitude. *Behav. Genet.* **37**, 273–283 (2007).

49. W. M. Compton, G. J. Dowling, H. Garavan, Ensuring the Best Use of Data. *JAMA Pediatr.* (2019) https:/doi.org/10.1001/jamapediatrics.2019.2081 (August 29, 2019).

50. H. Garavan, *et al.*, Recruiting the ABCD sample: Design considerations and procedures. *Dev. Cogn. Neurosci.* **32**, 16–22 (2018).

51. B. A. Eriksen, C. W. Eriksen, Effects of noise letters upon the identification of a target letter in a nonsearch task. *Percept. Psychophys.* **16**, 143–149 (1974).

52. R. K. Heaton, *et al.*, Reliability and validity of composite scores from the NIH Toolbox Cognition Battery in adults. *J. Int. Neuropsychol. Soc.* **20**, 588–98 (2014).

53. N. Akshoomoff, *et al.*, VIII. NIH Toolbox Cognition Battery (CB): composite scores of crystallized, fluid, and overall cognition. *Monogr. Soc. Res. Child Dev.* **78**, 119–132 (2013).

54. M. H. Daniel, D. Wahlstrom, O. Zhang, "Equivalence of Q-interactive™ and Paper Administrations of Cognitive Tasks: WISC ®-V Q-interactive Technical Report 8" (2014).

55. W. Acker, *A computerized approach to psychological screening—The Bexley-Maudsley*

Automated Psychological Screening and The Bexley-Maudsley Category Sorting Test (1982).

56. D. Weschler, *Weschler Intelligence Scale for Children, 5th ed* (Pearson, Bloomington, MN, 2014).

57. M. D. Tisdall, *et al.*, Volumetric navigators for prospective motion correction and selective reacquisition in neuroanatomical MRI. *Magn. Reson. Med.* **68**, 389–399 (2012).

58. N. White, *et al.*, PROMO: Real-time prospective motion correction in MRI using image-based tracking. *Magn. Reson. Med.* **63**, 91–105 (2010).

59. B. J. Casey, *et al.*, The Adolescent Brain Cognitive Development (ABCD) study: Imaging acquisition across 21 sites. *Dev. Cogn. Neurosci.* **32**, 43–54 (2018).

60. D. J. Hagler, *et al.*, Image processing and analysis methods for the Adolescent Brain Cognitive Development Study. *Neuroimage*, 116091 (2019).

61. B. Fischl, M. I. Sereno, A. M. Dale, "Cortical Surface-Based Analysis II: Inflation, Flattening, and a Surface-Based Coordinate System" (1999).

62. A. M. Dale, B. Fischl, M. I. Sereno, Cortical Surface-Based Analysis. *Neuroimage* **9**, 179–194 (1999).

63. B. Fischl, A. M. Dale, Measuring the thickness of the human cerebral cortex from magnetic resonance images. *Proc. Natl. Acad. Sci. U. S. A.* **97**, 11050–11055 (2000).

64. B. Fischl, *et al.*, Sequence-independent segmentation of magnetic resonance images. *Neuroimage* **23**, S69--S84 (2004).

65. J. Jovicich, *et al.*, Reliability in multi-site structural MRI studies: Effects of gradient non-linearity correction on phantom and human data. *Neuroimage* **30**, 436–443 (2006).

66. A. M. Winkler, M. A. Webster, D. Vidaurre, T. E. Nichols, S. M. Smith, Multi-level block permutation. *Neuroimage* **123**, 253–268 (2015).

67. A. M. Winkler, G. R. Ridgway, M. A. Webster, S. M. Smith, T. E. Nichols, Permutation inference for the general linear model. *Neuroimage* **92**, 381–397 (2014).

68. D. Freedman, D. Lane, A Nonstochastic Interpretation of Reported Significance Levels. *J. Bus. Econ. Stat.* **1**, 292 (1983).

FIGURES

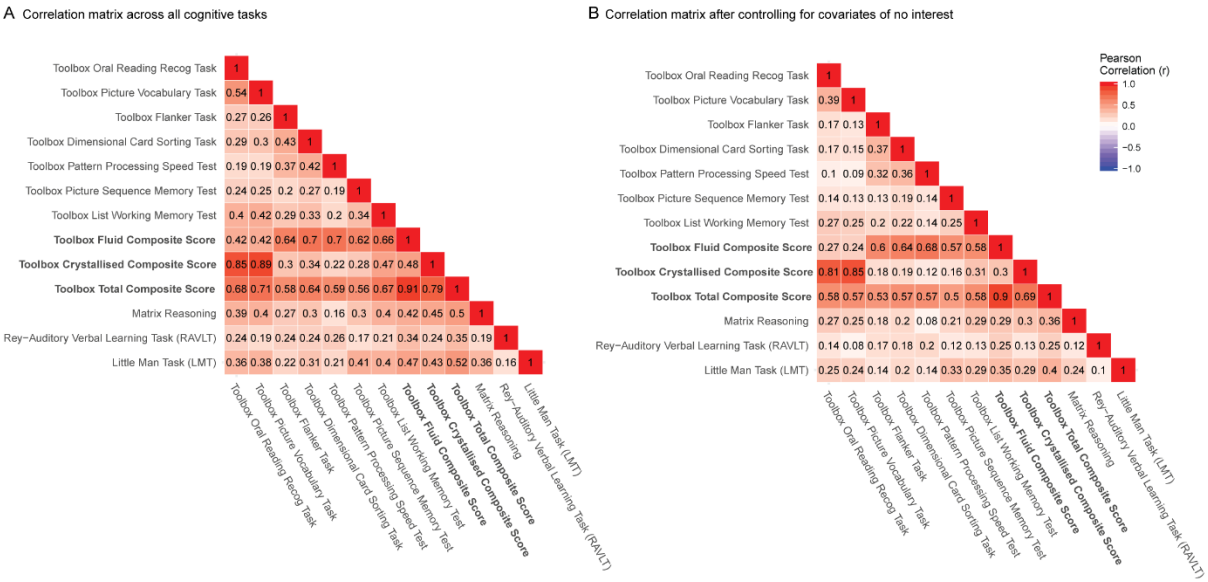

Figure 1. Phenotypic correlations between all of the cognitive measures at baseline in ABCD. A) Pearson correlation coefficients for all cognitive tasks. B) Correlations after controlling for covariates of no interest (age, sex, race/ethnicity, household income, parental education, scanner). Cognitive performance was pre-residualised for all covariates and then correlated using a Pearson correlation. Darker colours indicate a higher correlation coefficient. The composite scores are highlighted in bold. The other cognitive measures are single tasks. Correlation coefficients among the single task measures decreased after controlling for the covariates of no interest demonstrating that these additional measures explained a proportion of the variance in cognitive performance among these tasks.

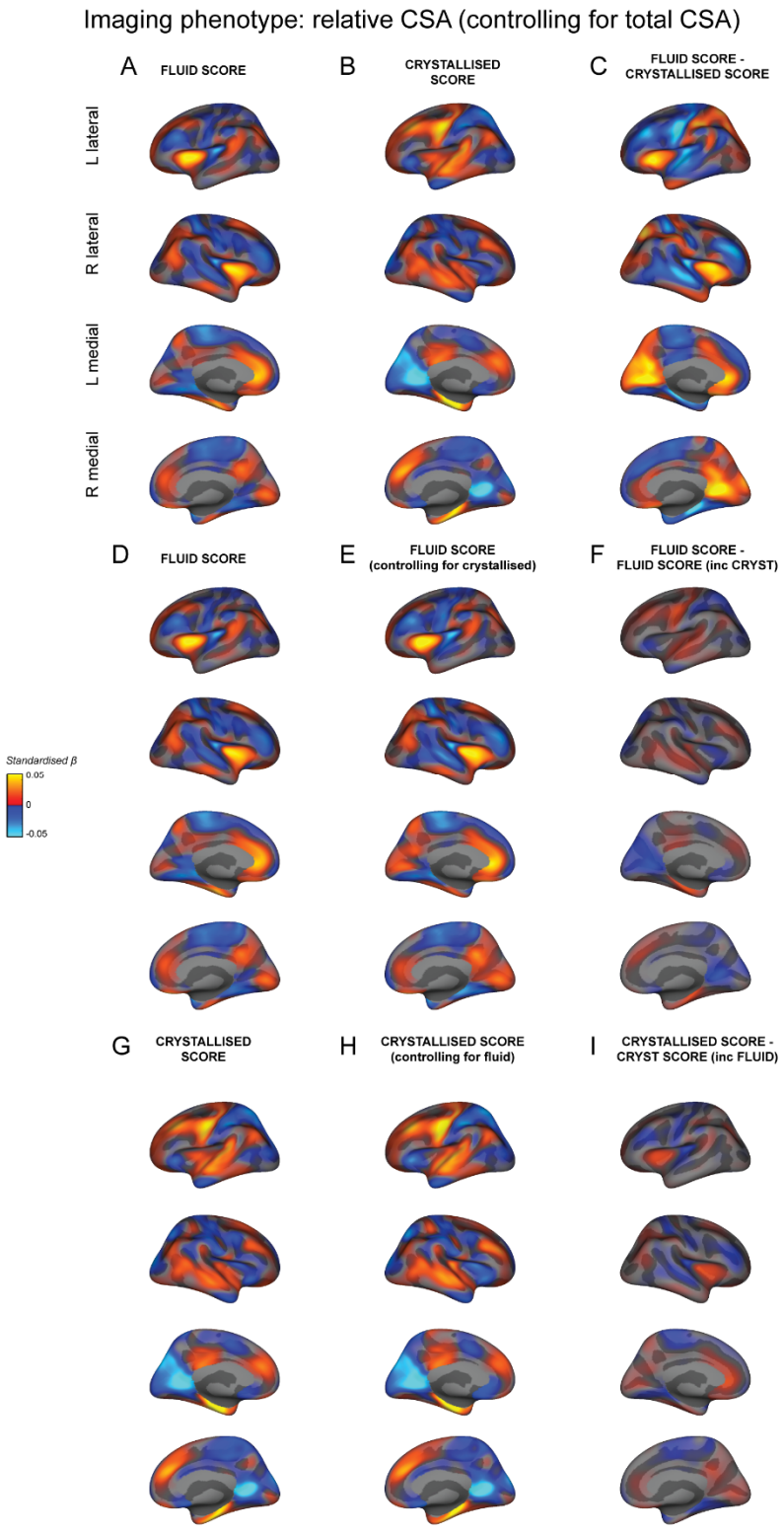

Figure 2. Distinct estimated effect size maps of association between the regionalisation of CSA and fluid and crystallised composite scores. All maps display the vertex-wise mass univariate standardised beta coefficients unthresholded for each association. A+D) The association between relative CSA and the fluid composite score and (B+G) the crystallised composite score. C) The difference in standardised beta coefficients between A+B. E) The association between relative CSA and the fluid composite score controlling for the crystallised composite score. F) The difference in standardised beta coefficients between D+E. H) The association between relative CSA

and the crystallised composite score controlling for the fluid composite score. I) The difference in standardised beta coefficients between G+H. The estimated effect size maps showing the association between the regionalisation of CSA and the fluid and crystallised composite scores have distinct patterns. These behavioural measures show very little overlapping variance with the regionalisation of CSA.

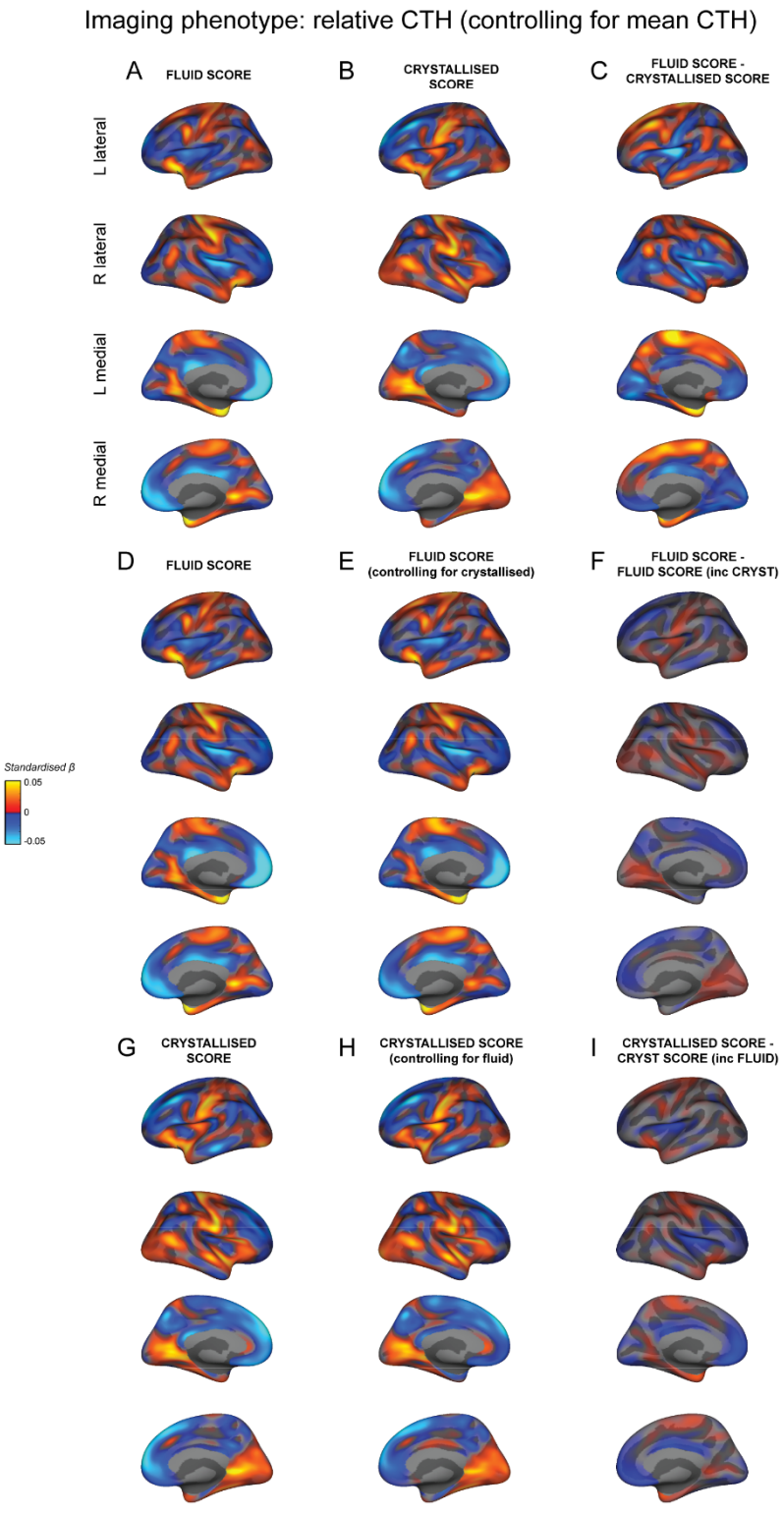

Figure 3. Distinct estimated effect size maps of association between the regionalisation of CTH and fluid and crystallised composite scores. All maps display the vertexwise mass univariate standardised beta coefficients unthresholded for each association. A+D) The association between relative CTH and the fluid composite score and (B+G) the crystallised composite score. C) The difference in standardised beta coefficients between A+B. E) The association between relative CTH and the fluid composite score controlling for the crystallised composite score. F) The difference in standardised beta coefficients between D+E. H) The association between relative CTH and the crystallised composite score controlling for fluid composite score. I) The difference in standardised beta coefficients between

G+H. The estimated effect size maps showing the association between the regionalisation of CTH and the fluid and crystallised composite scores have distinct patterns. These behavioural measures show very little overlapping variance with the regionalisation of CTH.

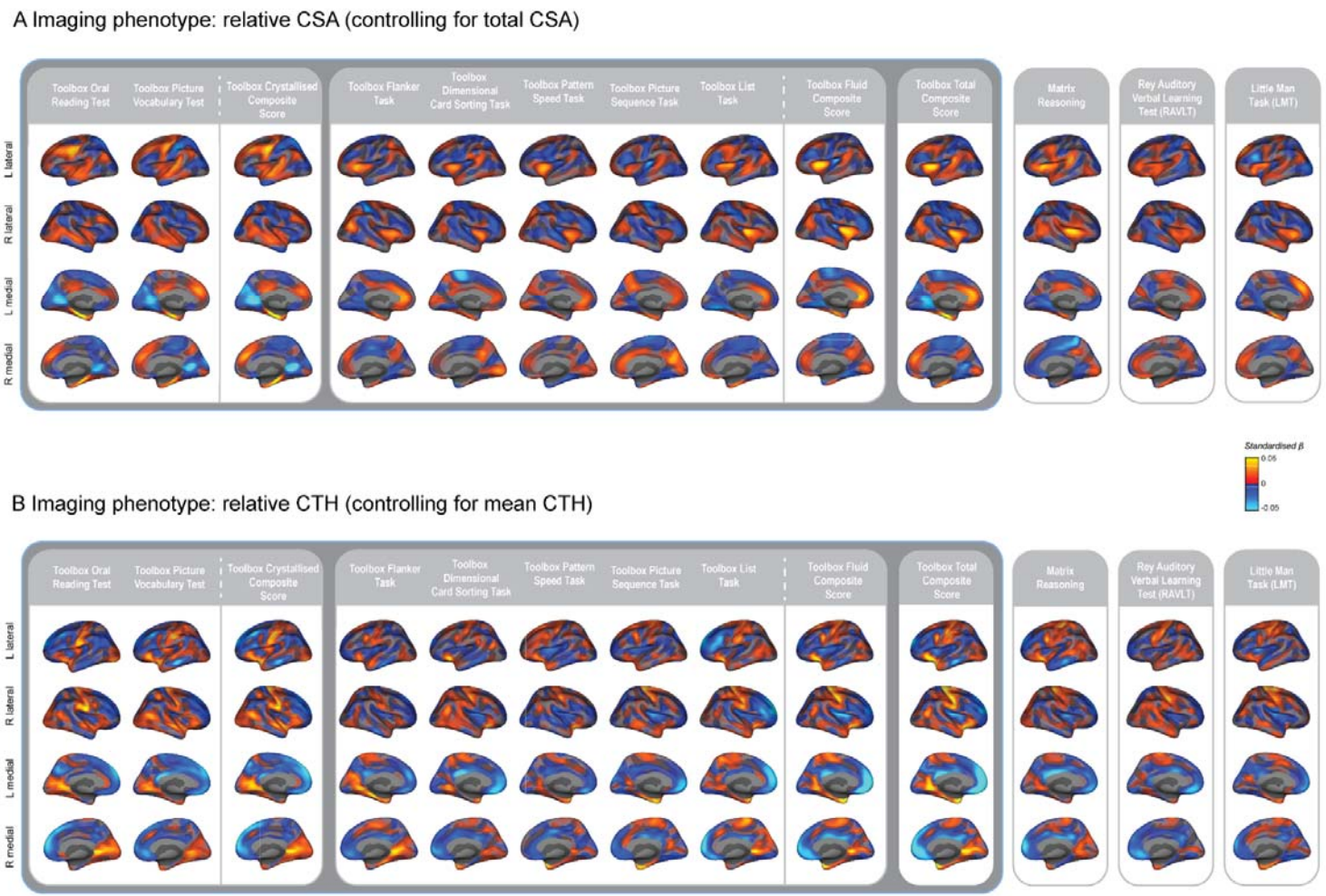

Figure 4. Estimated effect size maps showing the mass univariate standardised beta coefficients for the association between each cognitive task and (A) the regionalisation of CSA and (B) the regionalisation of CTH. Performance on all of the cognitive tasks and the composite scores showed significant associations with the regionalisation of cortical morphology across the whole cortical surface according to the MOSTest as determined in Palmer et al (2019).

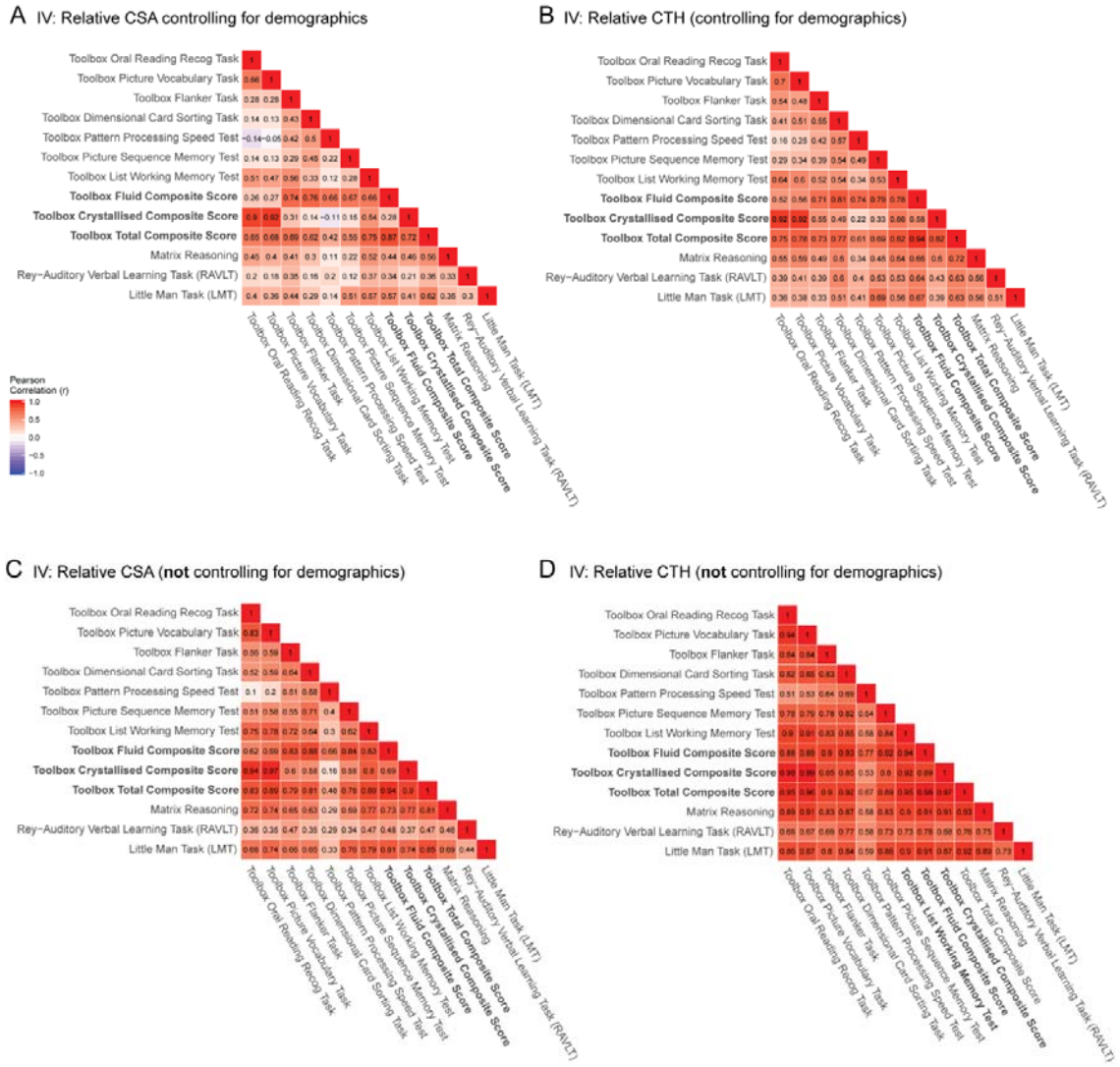

Figure 5. Similarity of regionalisation association patterns across cognitive tasks is modulated by demographic factors. Pairwise vertex-wise correlations between the estimated beta coefficients across all cognitive tasks predicted by A) the regionalisation of CSA and B) the regionalisation of CTH controlling for the demographic variables of race/ethnicity, household income and parental education. C&D) Pairwise vertex-wise correlations for all of the cognitive tasks and C) the regionalisation of CSA and D) the regionalisation of CTH not controlling for the specified demographic variables. The correlation amongst associations was much larger when these demographic variables were not included in the GLMs used to produce the estimated effect size maps.

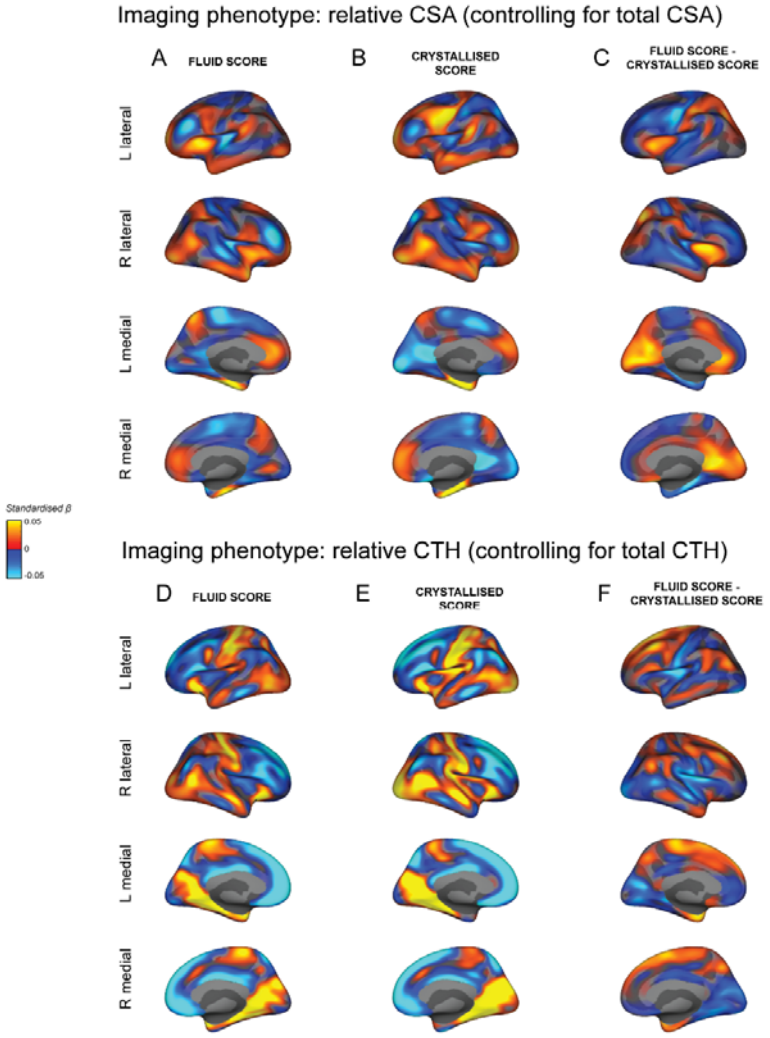

Figure 6. Similar estimated effect size maps for the association between the regionalisation of cortical morphology and the fluid and crystallised composite scores when <u>not</u> controlling for demographic factors. All maps display the vertex-wise mass univariate standardised beta coefficients unthresholded for each association. The top part of the figure shows the association between the regionalisation of CSA and the fluid composite score (A) and the crystallised composite score (B). C) The difference in standardised beta coefficients between A+B. The bottom part of the figure shows the association between the regionalisation of CTH and the fluid composite score (D) and the crystallised composite score (E). F) The difference in standardised beta coefficients between D+E. The demographic variables of race/ethnicity, household income and parental education were not included in the mass univariate GLMs to produce these estimated effect size maps. The exclusion of these confounding factors increased the magnitude of the estimated beta coefficients and the similarity between the maps for the fluid and crystallised composite scores. However, the difference maps (C+F) closely reflect the pattern of differences seen in figure 2C and figure 3C respectively.

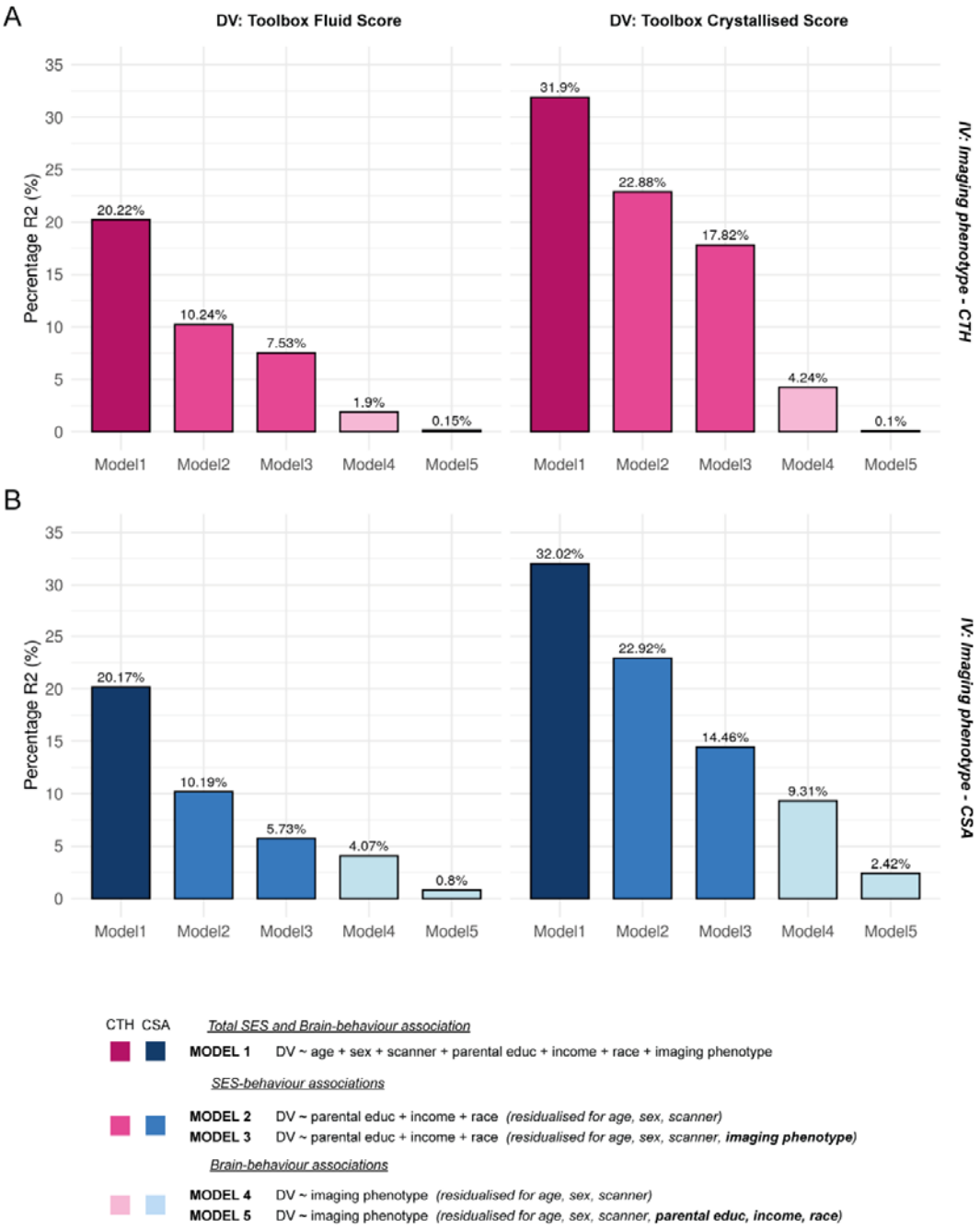

Figure 7. Controlling for sociodemographic factors reduces the variance in cognitive performance predicted by cortical morphology. These bar charts show the percentage R^2 in the crystallised (left column) and fluid (right column) composite scores predicted by several models including sociodemographic and brain measures. Model 1 shows the total variance in behaviour explained by the full model including the covariates of no interest (age, sex and scanner), the sociodemographic variables (parental education, household income and race/ethnicity) and either the regionalisation of CTH and mean CTH (A; pink) or the regionalisation of CSA and total CSA (B; blue). Model 2 shows the *unique* variance in behaviour explained by the sociodemographic factors after pre-residualising both the dependent (DV) and independent (IV) variables for the covariates of no interest. Additionally, pre-residualising for the imaging phenotypes (model 3) lead to a reduction in this R^2. Conversely, model 4 shows the *unique* variance in behaviour explained by the structural measures (global below the dotted line; and regionalisation above the dotted line) after pre-residualising for the covariates of no interest only. Additionally pre-residualising for the sociodemographic factors (model 5) lead to a large decrease in the variance explained by these structural measures, again showing the shared variance between these measures. Controlling for the sociodemographic factors of race/ethnicity, household income and parental education reduced the variance explained in the composite scores by ~4-5 fold for CSA and ~4-8 fold for CTH.